Fachtagung "Lasermethoden in der Strömungsmesstechnik"
4. – 6. September 2012, Rostock

EXPERIMENTS ON THE INTERACTION OF WIND GUSTS AND FOREST EDGES

EXPERIMENTELLE UNTERSUCHUNGEN ZUR INTERAKTION VON WINDBÖEN UND WALDKANTEN

M. Tischmacher, B. Ruck
Laboratorium für Gebäude- und Umweltaerodynamik, Institut für Hydromechanik,
Karlsruher Institut für Technologie (KIT), Kaiserstrasse 12, 76128 Karlsruhe

Forest edge, gust, TR-PIV, wind tunnel experiments

Abstract

Observations in nature suggest a particularly high risk of wind-induced forest damage in the near-edge region. Unsteady processes excited by strong gusts from the atmospheric boundary layer are likely to play a major role. To gain more insight into the corresponding flow behaviour, wind tunnel experiments were made with artificially generated 3D wind gusts, produced by short inductions of pressurized air, combined with Time Resolved - Particle Image Velocimetry measurements. The interactions of forest edges of different shape with unsteady gusts were investigated. The findings show that an edge-induced primary vortex, which forms shortly behind the edge, 'catches' high momentum fluid from the overflowing gust and directs it into the canopy. It seems that this primary vortex forms when a gust passes the forest edge and the upper part of the gust overflows the edge whereas the lower part penetrates the forest front. The fluid mass entering the forest front is decelerated and leaves the canopy top leading to a kind of cross flow phenomenon with the overflowing part of the gust. As a result, the primary vortex is generated, which is then subject to typical Kelvin-Helmholtz instability condition.

1. Introduction

Flow above and through vegetation has been of high interest since many years and the motivations to work on this topic are manifold (de Langre 2008). Especially on the interaction of airflow and trees and in particular on the wind-induced damage of forests much research has been accomplished and should be done in the future (Schindler et al. 2012). One reason for this research are winter storms, which have the most destructive potential of all natural risks for European forests (Albrecht et al. 2010). Schelhaas et al. (2003) reported that in the period from 1950 to 2000 storms were responsible for 53% of total damage of European forests which is about 8.1% of the total fellings in Europe and Henneka et al. (2006) found that storms are by far the costliest natural catastrophes in Germany.

From many observations it is known that wind-related damage to trees is often associated with hilly topography or canopy heterogeneity such as edges and clearings (Finnigan and Brunet 1995). Of particular interest has been the flow at windward forest edges as sometimes the damage occurs some distance behind the first row (Mitscherlich 1971). But already

Wölfle (1937) stated that this phenomenon can not be explained only by the fact that the first tree rows grow more windfirm than trees inside the stand. Still today, the dynamics of the air flow at forest edges with respect to tree failure is not completely understood. In the last years special attention was given to the adjustment of the flow to the step change in surface roughness and the shear layer region which forms at canopy top (field experiments: Kruijt et al. 1995, Irvine et al. 1997; wind-tunnel experiments: Ruck and Adams 1991, Stacey et al. 1994, Morse et al. 2002, Agster and Ruck 2003, Ruck et al. 2010; numerical simulations: Yang et al. 2006, Dupont and Brunet 2008, 2009).

The specific literature shows agreement on the point that the process of wind-induced damage is unsteady. Coherent structures and less organized turbulent behaviour seem to play a major role for that process. Large Eddy Simulations provide much data and highly interesting results due to their ability of simulating unsteady processes with a three dimensional spatial resolution. But it is very important to conduct as well experiments in the field and in the laboratory to obtain equivalent insight on the dynamics of the flow and to validate the modelling assumptions made in the simulations. From this point of view we have been motivated to do Time Resolved Particle Image Velocimetry (TR-PIV) measurements at the Laboratory of Building and Environmental Aerodynamics, Institute for Hydromechanics, KIT in Karlsruhe (Germany). We focused on the unsteady processes which are most likely responsible to cause damage in the near-edge region of forests, i.e. the impact of a strong gust of the turbulent atmospheric boundary layer. The wind tunnel facility and the experimental setup allowed to do these experiments with a reproducibility and level of control which is not achievable in the field. It is our aim to gain and provide a deeper insight of the unsteady flow behaviour at forest edges with wind conditions likely to cause damage.

2. Experimental Details

2.1 Experimental Setup

The experiments were made in a closed-return wind tunnel (Goettinger type) and by Hot-wire and Laser Doppler anemometry the turbulence intensity of the wind tunnel was determined to be less than 2%. The working section of the tunnel is 3.30 m long with a 0.75 m * 0.75 m cross section of the nozzle. Behind the nozzle an extension of 1.11 m length was attached, so that a 90°-curved injection pipe could be inserted at the bottom. The injection pipe pointing towards the working section was connected to a fast pneumatic valve (FESTO solenoid valve MHE4-MS1H-3/2G-QS-8-K). The pneumatic valve itself was connected to a pressurized tank adjusted to a constant pressure of 4 bar throughout the experiments. The injection pipe had an inner diameter of 10 mm and the simulated gusts were released at height z_{pipe} = 11.5 cm, see figure 1. With the controllable valve and via the injection pipe, defined pulses of pressurized air (gusts) could be produced overlaying the base flow of 8 m/s. The opening time of the pneumatic valve was set to 16 ms throughout the experiments to produce strong gusts approaching the forest edge.

Field investigations as well as numerical simulations, see Choi 2004, Chay et al. 2006 a,b, Panneer Selvam and Holmes 1992, show that wind profiles of severe gusts, downbursts or thunderstorm gusts do not show a monotonically increasing wind speed with height but show a velocity maximum near the gust front nose. Apparently, an approaching severe gust overrules any wind characteristics of the base flow. Thus, in the present study, we omitted a detailed simulation of the atmospheric boundary layer profile of the base flow, i.e. no additional turbulence generating devices like spires or roughness elements were positioned in the

fetch. We concentrated solely on the interaction of single and defined severe gusts with a permeable forest edge. For the investigation and scaling of the artificial gust, measurements without a forest downstream of the pipe were performed as well.

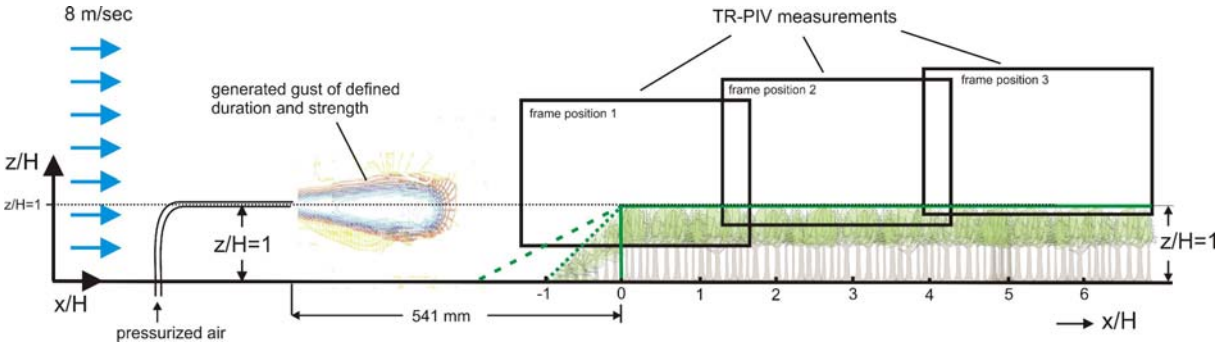

Fig. 1: Schematic of the experimental setup. A forest model of height H =11.5 cm was placed in the open test section of the wind-tunnel. Upstream of the forest edge, in a distance of 541 mm and in a height of $z_{pipe} = H$ = 11.5 cm, the injection pipe was positioned and connected to pressurized air via a controllable pneumatic valve.

For the experiments of the interaction of gusts and forest edges a forest model consisting of individual stiff conifer models of average height H =11.5 cm was placed 54.1 cm behind the outlet of the injection pipe. The tree models had a stream-wise and cross-wise spacing of 2 cm and a round 5.5 cm long and 4 mm thick polystyrene stem with a 6 $\pm$0.5 cm long crown. For measurements with different edge taper angles two different forest edges were mounted in front of the sharp 90°-forest edge (labeled TA90) with an inclination of 45° (TA45) and 27° (TA27), see figure 2.

Fig. 2: Windward side of model forest consisting of individuale 11.5 cm high conifer models, regularly spaced in stream-wise x and cross-wise y direction.

2.2 Measurement technique

Velocity measurements were made with a 2D/2C TR-PIV system of DantecDynamics. The TR-PIV system used for the experiments consisted of two frequency doubled Nd:YAG lasers (each 14 mJ/pulse at a frequency of 1000 Hz in Q-switch mode and wavelength of 532 nm) a high speed camera (SpeedSense9072, 2190 frames per second at full resolution, 32 GB memory) with a 1280*800 pixel CMOS-Sensor (pixel-size px^2 = 20*20 µm^2) and a Zeiss Planar T* 1.4/50mm ZF lens. The laser beams were aligned by mirrors, adjusted by cylindrical lenses and directed into the working section by a mirror to illuminate the measurement positions with a 1 mm thick light sheet. The tracer particles of 1-3 µm size were generated by vaporization and condensation of 1,2-propanediol and injected at the end of the working section to ensure a homogeneous seeding of the air. A digital synchronizer was utilized to syn-

chronize the pneumatic valve and hence the artificial gust generation with the PIV measurements (see as well Tischmacher and Ruck 2011).

Three positions above the forest model were defined for 2D/2C TR-PIV measurements in the same plane as the pipe and directly above a line of trees. The measurement areas are all about 370 mm in width, 231 mm in height, hence corresponding to ratio of 0.29 mm/px, and cover the near-edge region from -1.29 x/H to 6.98 x/H, compare figure 1.

The measurements where made with a sampling frequency of 1000 Hz in the double frame/single exposure mode (Raffel et al. 2007). Afterwards the particle images were evaluated with the software DynamicStudio v3.00 of DantecDynamics using an adaptive cross-correlation algorithm with 50% overlap to obtain the velocity vectors which were validated with a peak-height criterion of 1.2 and a median filtering on 3*3 IAs. The final size of the IAs was $32\,px$*$32\,px$ corresponding to a spatial resolution of about 9.2 mm*9.2 mm = $0.08\,H$*$0.08\,H$. To correct the low but systematic error of the lens distortion, a calibration with a third order polynomial was applied to the velocity vectors which were afterwards exported to MATLAB for post-processing.

2.3 Analysis

The synchronization allowed for calculating the ensemble average of different gust events which will be denoted by angular brackets in the following, e.g.

$$\langle u \rangle(x,z,t) = \frac{1}{N}\sum_{k=1}^{N} u_k(x,z,t)$$

for the horizontal velocity component u, but equivalently for the vertical component w or for the ensemble averaged momentum flux $\langle uw \rangle$. At each measurement position and for each edge shape setup, 54 gust events were injected and measured for 300 ms.

To analyse the measured process, it proved valuable to extract information on the vortical structure of the ensemble averaged velocity field. The identification of vortices in turbulent flows is not straight-forward (Jeong and Hussain 1995) and vorticity fails in general to detect a swirling motion. As identification of vortical motion the swirling strength

$$\lambda_{ci}^2 = \frac{1}{4}\left(\frac{\partial u}{\partial x}\right)^2 + \frac{1}{4}\left(\frac{\partial w}{\partial z}\right)^2 - \frac{1}{2}\frac{\partial u}{\partial x}\frac{\partial w}{\partial z} + \frac{\partial u}{\partial z}\frac{\partial w}{\partial x}$$

was used as defined in Zhou et al. (1999) and Adrian et al. (2000). In the case of swirling motion, the value λ_{ci}^2 is negative whereas a higher absolute value indicates a stronger rotational motion.

3. Results

3.1 Gust characteristics

The gusts were produced by injecting pressurized air for a duration of 16 ms into a base flow. Figure 3 shows a typical gust generated in the wind tunnel. The gust contours are ensemble averaged over 50 individual gusts, released at a height z/H = 1.4 and without a forest

model in the test section downstream of the injection pipe (pure approach flow). As can be seen, the gust is accompanied by a vortex ring structure. The gusts, which effect we want to describe in this article, were released at height z/H = 1. The gust factor of 1.6 and a corresponding length of about 3.2*H indicates a strong and in nature rarely occurring gust (Deacon 1965).

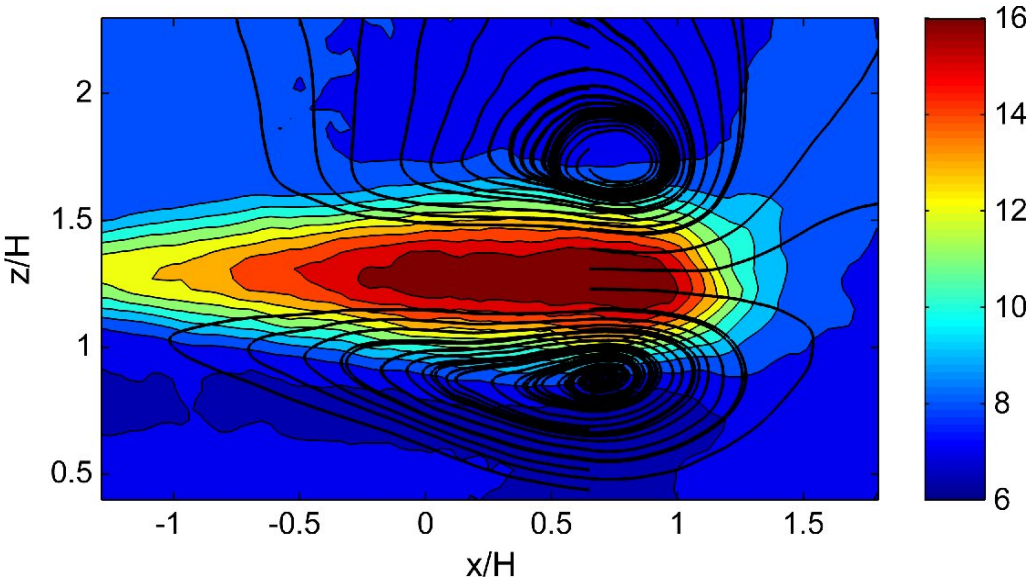

Fig. 3: Structure of the ensemble average of 50 gusts released at height 1.4H . The colour coding represents $\langle u \rangle$ in absolute values, [m/s], and the streamlines are calculated by the velocity field $\left(\langle u \rangle - u_{ref}, \langle w \rangle\right)$ with the free-stream velocity u_{ref} = 8 m/s.

3.2 The base flow

The gusts were released into a low turbulence base flow which is characterized in figure 4. The velocity vectors show the upward deflection and distortion of the flow as well as the strong deceleration close above the canopy. The most rapid deceleration occurs in the range of the first two tree heights, which is as well the region where – as expected – a pronounced upward outflow due to continuity is present.

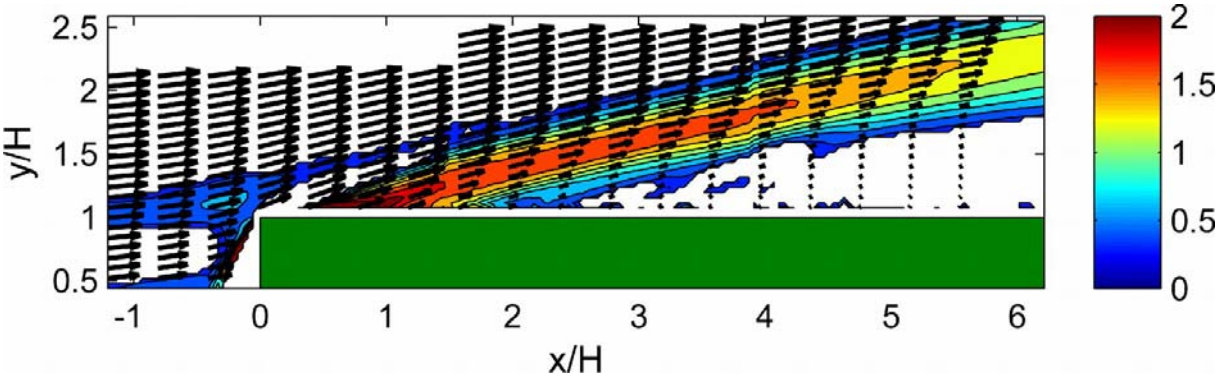

Fig. 4: Setup TA90; mean velocity vectors for the base flow with corresponding colour-coded horizontal mean velocity shear $\partial\overline{u}/\partial z \cdot H/u_{ref}$. Values lower than 0.3 are blanked for a better visibility of the shear layer.

The contours of the normalized shear reveal a thin shear layer (wake) caused by the presence of the injection pipe in front of the model at height H and the existence of a second strong shear layer which originates at canopy top height of the forest at $0 < x/H < 1$. In contrast to the findings of canopy flows in a simulated and scaled atmospheric boundary layer, we see that the shear layer detaches downstream of its origin and its inflection point height is not at canopy top but is increasing with x. But we think that this is of minor importance, as the strong momentum of the artificial gust dominates such that this difference is negligible for the dynamical behaviour.

3.3 Dynamics of the gust at the forest edge

The induction of pressurized air into a base flow causes a correlated air packet with overspeed, i.e. a gust to approach the forest edge. The structure of the gust is like an elongated vortex ring and as the injection pipe is located at $z = H$ we see in the measuring plane a counter-clockwise rotating vortex above $z = H$ and a clockwise rotating vortex below $z = H$. The two the forest edge approaching rotational cores can be seen in figure 5 a, which shows the swirling strength of the ensemble averaged flow velocity field as well as the corresponding velocity vectors. As the gust approaches the forest, the lower vortex is not lifted above the edge but impinges on the first tree row. The upper vortex instead is deflected upwards and the velocity is strongly increased above the canopy directly at the edge during the gust passage, as can be seen in figure 5 b. In the following, a vortex core starts to develop at the canopy top in the region of $1 < x/H < 2$, see figure 5 c.

The new forming canopy top vortex seems to be initiated by the cross flow of high momentum gust fluid over the canopy and an upward outflow from below. This upward flow out of the canopy is observable until about 1.5 x/H and is caused by fluid mass entering the stem area at the frontal edge. As a consequence of a deceleration in the stand, fluid mass is forced to leave the forest at the canopy top. It seems that fluid mass coming out of the canopy leads to a classical cross flow phenomenon resulting in the primary vortex, which, then, is subject to plane mixing layer instabilities. The swirling motion associated with the primary vortex shortly behind the forest edge at canopy top height is increasing in size and causes momentum to be transported into the tree crowns in front of its moving core, see figure 5 c,d. Downstream of about four tree heights behind the first tree row, the swirling strength decreases whereas the size of the rotational area is growing and losing its clear structure, see figure 5 e.

Figure 6 shows for the three different forest edge configurations the most negative values of the ensemble averaged momentum flux. Just negative values are plotted, indicating regions of strong downward directed motion and hence regions of an increased forest damage probability. Due to figure 6 the TA45 and TA27 configurations indicate that the region of strongest downward momentum flux is shifted by tapered edges to about one tree height upstream compared to the TA90 configuration. Although the region of a strong impact is more pronounced in the TA45 case, the greatest magnitude at height $z = 1.16H$ is almost equal for the TA27 and TA45 configuration and is about 12% more negative than for the TA90 configuration. The region where negative values of $\langle uw \rangle$ occur covers – at least for $x > 2H$ - the part below the shear layer indicating line of the base flow (compare figure 4).

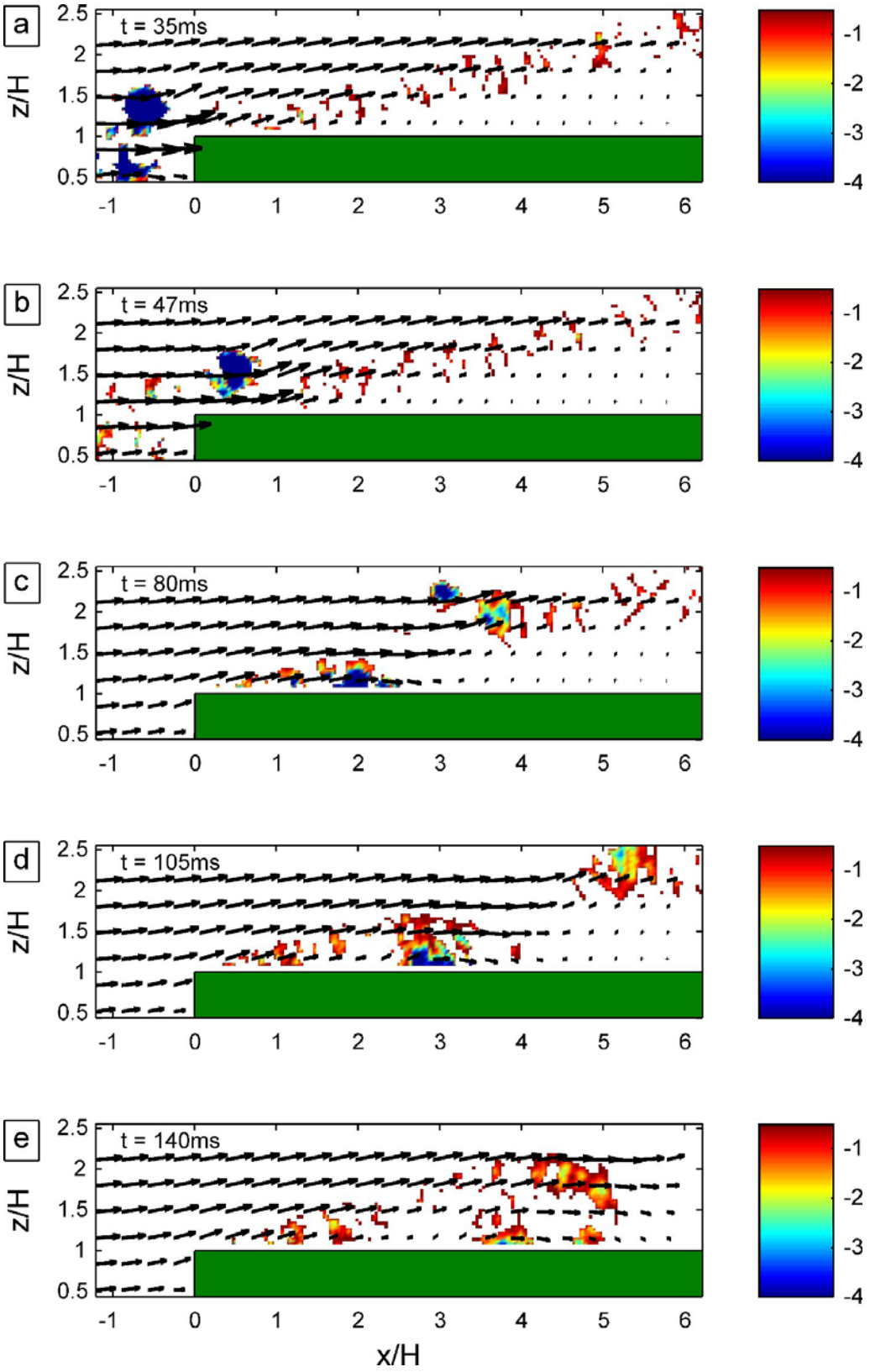

Fig. 5: Colour-coded swirling strength, $1000\,\lambda_{ci}^2$, and velocity vectors of the ensemble averaged flow field at 5 different times w.r.t. the opening time of the pneumatic valve. All vector lengths of the figure are plotted at the same scale. Values above -250 of the swirling strength are blanked out.

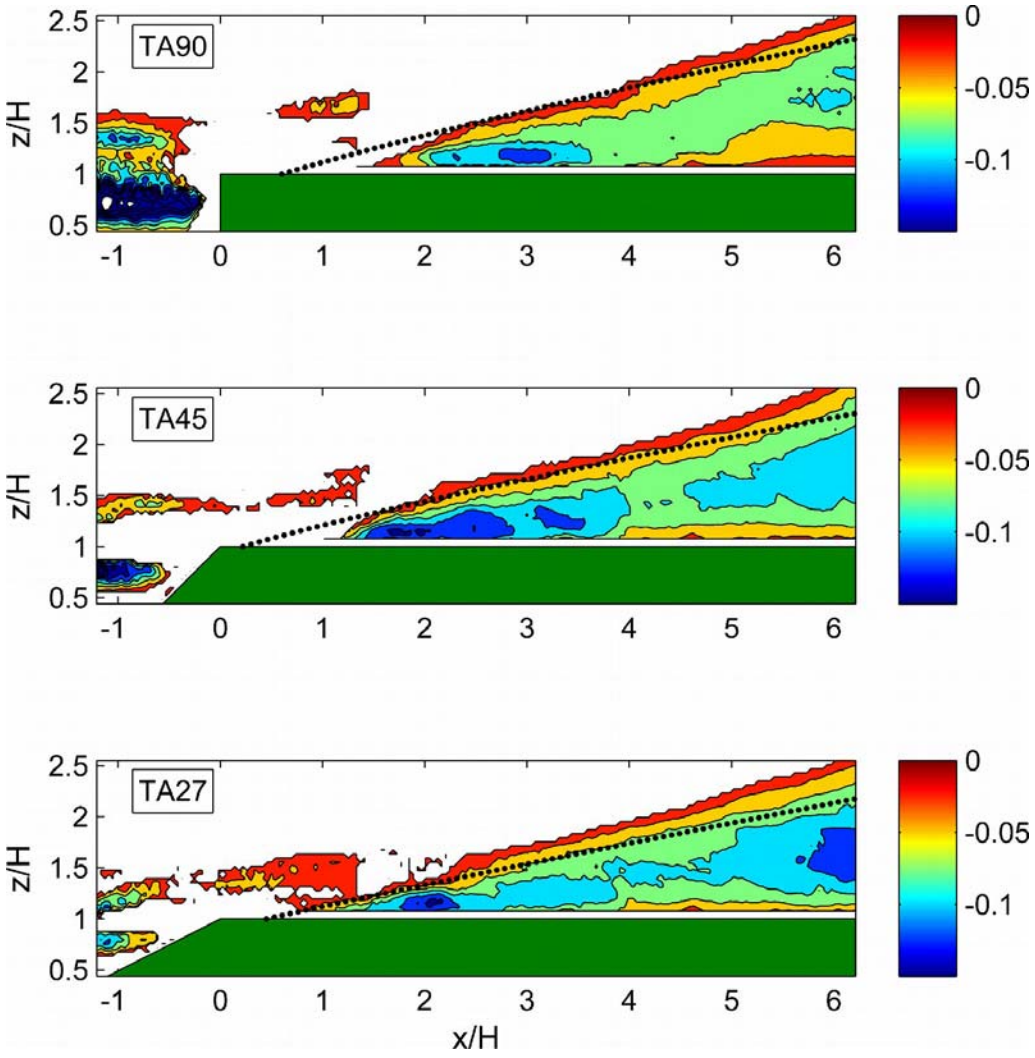

Fig. 6: Negative $\langle uw \rangle$-values by 54 gust events for the setups TA90, TA45 and TA27, gusts released at height $z_{pipe} = H$. Plotted are the normalized most negative values of $\langle uw \rangle$ of the gust event. The dotted lines represent the middle of the corresponding detached shear layers of the undisturbed flow (see fig. 4).

4. Discussion and Conclusion

The TR-PIV measurements revealed the gust dynamics with a so far unknown spatial and temporal resolution. We found in detail that a part of the gust penetrates the forest front (edge), whereas another part continues its way over the canopy. Fluid mass, which penetrates the forest front is partially blocked by stems and canopy material. Thus, as a consequence of continuity, a part of the inflow mass flows out via the canopy top within a distance of about 1-2 tree heights from the edge. When the first outflow takes place during a gust event, the gust is still blowing over the edge provided that it has a certain length. We found, that the interference of canopy outflow and horizontal flow of that gust part, which passes the edge-region above canopy height, induces the development of a swirling motion (clockwise if the flow is from left to right) at canopy top between 1 and 2 x/H. This is the onset region for a primary vortex. The outflowing fluid mass induces an instability (cross flow-like) in the flow field above the edge-near canopy, which leads to the formation of the primary vortex. The formation at canopy top starts beneath the overflowing gust, i.e. only the front portion of the

gust has past the location of the primary vortex formation. Thus, the rest of the gust is affected by the primary vortex, which catches high speed fluid from the gust center and directs it into the canopy. All this indicates that the gust length as well as the strength of the primary vortex play an important role for the problem and have to be considered.

Furthermore, the findings show that the formation of the primary vortex, which can also be referred to as 'first large coherent structure behind the edge', is rather a cross flow phenomenon than a pure Kelvin-Helmholtz-type instability phenomenon. However, both phenomena overlap and it is not surprising that LES computations without discrete severe gust simulation (Dupont and Brunet 2009) deliver at least qualitatively comparable results. The presented results suggest that for severe gusts the plane mixing layer analogy (see Finnigan and Brunet 1995, Raupach et al. 1996, Finnigan 2000) cannot be used alone to explain the formation of the primary vortex. We are convinced that the primary vortex is initiated by the interference of the described edge-near canopy outflow and the overflowing part of the gust. After the formation, the vortex is advected downstream and, of course, subject to mixing layer conditions.

LDA experiments with different edge taper angles (Ruck et al. 2010) indicate an upstream shift of the area of high turbulent momentum fluxes for decreasing taper angle. This agrees with the findings of the unsteady PIV experiments (see fig. 6). However, a fundamental and qualitative difference of the outer flow field induced by forest edges with different angles was not measured.

Acknowledgements

The authors thank the Deutsche Forschungsgemeinschaft DFG/Bonn for the financial support within the project Ru-345/30-1 "Die hochinstationäre Wechselwirkung zwischen Windböen und Waldkanten".

Literature

Adrian, R. J., Christensen, K. T., Liu, Z.-C., 2000, Analysis and interpretation of instantaneous turbulent velocity fields, *Exp. Fluids* 29: 275-290

Agster, W., Ruck, B., 2003, The influence of aerodynamic properties of forest edges and stands on the pressure pattern within a forest, in: Ruck, B., Kottmeier, C., Mattheck, C., Quine, C., Wilhelm, G., (Eds.), *Proc. Intern. Conf.* Wind Effects on Trees, 2003, pp. 25-32

Albrecht, A., Hanewinkel, M., Bauhus, J., Kohnle, U., 2010, How does silviculture affect storm damage in forests of south-western Germany? Results from empirical modelling based on long-term observations, *Eur. J. Forest Res.* 131: 229-247

Chay, M.T., Albermani, F., Hawes, H., 2006a, Wind Loads on Transmission Line Structures in Simulated Downbursts. In: *First World Congress on Asset Management*, Gold Coast, Australia

Chay, M.T., Albermani, F., Wilson, R., 2006b, Numerical and analytical simulation of downburst wind loads, *Engineering Structures* 28: 240-254

Choi, E.C.C., 2004, Field measurements and experimental study of wind speed profile during thunderstorms, *J. Wind Eng. Ind. Aerodyn.* 92: 275-290

Deacon, E. L., 1965, Wind gust speed: averaging time relationship, *Aust. Met. Mag.* 51: 11–14

De Langre, E., 2008, Effects of wind on plants, *Annu. Rev. Fluid Mech.* 40:141–68

Dupont, S., Brunet, Y. 2008, Edge Flow and Canopy Structure: A Large-Eddy Simulation Study, *Bound. Layer Meteorol.* 126: 51-71

Dupont, S., Brunet, Y. 2009, Coherent structures in canopy edge flow: a large-eddy simulation study, *J. Fluid Mech.* 630: 93-128

Finnigan, J. J., Brunet, Y., 1995, Turbulent airflow in forests, in: Coutts, M. P., Grace, J. (Eds.), Wind and Trees, 1995, Cambrigde University Press, Cambridge, UK, pp. 3-40

Finnigan, J., 2000, Turbulence in plant canopies, *Annu. Rev. Fluid Mech.* 32:519-517

Heneka, P., Hofherr, T., Ruck, B., Kottmeier, C., 2006, Winter storm risk of residential structures – model development and application to the German state of Baden-Württemberg, *Nat. Hazards Earth Syst. Sci.* 6: 721–733
Irvine, M. R., Gardiner, B. A., Hill, M. K., 1997, The evolution of turbulence across a forest edge, *Bound. Layer Meteorol.* 84: 467-496
Jeong, J., Hussain, F., 1995, On the identification of a vortex, *J. Fluid Mech.* 285: 69-94
Kruijt, B., Klaassen, W., Hutjes, R. W. A., 1995, Edge effects on diffusivity in the roughness layer over a forest, in Wind and Trees 1995, Coutts, M. P., Grace, J. (Editors)
Mitscherlich, G., 1971, Wald, Wachstum und Umwelt, Band 2: Waldklima und Wasserhaushalt. Sauerländer, Frankfurt a. M.: 365 S.
Morse, A. P., Gardiner, B. A., Marshall, B. J. 2002, Mechanisms controlling turbulence development across a forest edge, *Bound. Layer Meteorol.* 103: 227-251
Panneer Selvam, R., Holmes, J.D., 1992, Numerical simulation of thunderstorm downdrafts, *J. Wind Eng. Ind. Aerodyn.* 44: 2817–2825
Raffel, M., Willert, C., Wereley, S., Kompenhans, J., 2007, Particle Image Velocimetry: A Practical Guide, 2nd edition, Springer
Raupach, M. R., Finnigan, J. J., Brunet, Y. 1996, Coherent eddies and turbulence in vegetation canopies: the mixing-layer analogy, *Bound. Layer Meteorol.* 78: 351-382
Ruck, B., Adams, E., 1991, Fluid mechanical aspects in the pollutants transport to coniferious trees, *Bound. Layer Meteorol.* 56: 163-195
Ruck, B., Frank, C., Tischmacher, M., 2010, On the influence of windward edge structure and stand density on the flow characteristics at forest edges, *Eur J Forest Res* 131: 177-189
Schelhaas, M. J., Nabuurs, G. J., Schuck, A., 2003, Natural disturbances in the European forests in the 19th and 20th centuries, *Global Change Biology*, 9:1620-1633
Schindler, D., Bauhus, J., Mayer, H., 2012, Wind effects on trees, *Eur J Forest Res*, 131:159-163, DOI 10.1007/s10342-011-0582-5
Stacey, G. R., Belcher, R. E., Wood, C. J., Gardiner, B. A., 1994, Wind flows and forces in a model spruce forest, *Bound. Layer Meteorol.* 69: 311-334
Tischmacher, M., Ruck, B., 2011, Untersuchungen zur Böendynamik an Waldkanten, Proceedings der 19. Fachtagung „Lasermethoden in der Strömungsmesstechnik", Universität Ilmenau, 44, ISBN -3-9805613-7-2
Wölfle, M., 1937: Sturmschäden im Wald. II. Mitt. Forstwiss. Cent.bl. 59: 77–92
Yang, B., Shaw, R. H., Kyaw, T. P. U 2006, Wind loading on trees across a forest edge: a large eddy simulation, *Agric. For. Meteorol.* 141: 133-146
Zhou, J., Adrian, R. J., Balachandar, S., Kendall, T. M., 1999, Mechanisms for generating coherent packets of hairpin vortices in channel flow, *J. Fluid Mech.* 387: 353-396